

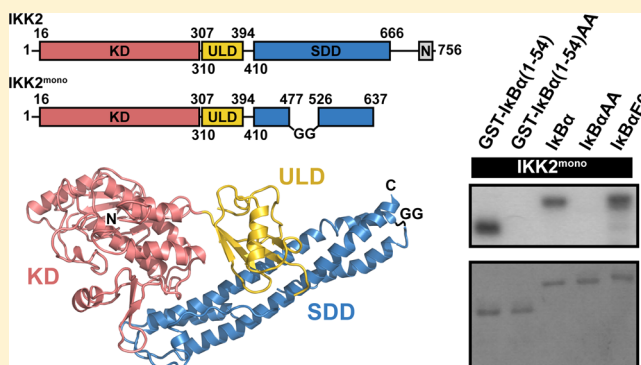
## Probing Kinase Activation and Substrate Specificity with an Engineered Monomeric IKK2

Arthur V. Hauenstein,<sup>†</sup> W. Eric Rogers,<sup>†</sup> Jacob D. Shaul,<sup>†,§</sup> De-Bin Huang,<sup>‡</sup> Gourisankar Ghosh,<sup>‡</sup> and Tom Huxford<sup>\*,†</sup>

<sup>†</sup>Structural Biochemistry Laboratory, Department of Chemistry & Biochemistry, San Diego State University, 5500 Campanile Drive, San Diego, California 92182-1030, United States

<sup>‡</sup>Department of Chemistry & Biochemistry, University of California–San Diego, 9500 Gilman Drive, La Jolla, California 92093-0357, United States

**ABSTRACT:** Catalytic subunits of the  $\kappa$ B kinase (IKK), IKK1/IKK $\alpha$ , and IKK2/IKK $\beta$  function *in vivo* as dimers in association with the necessary scaffolding subunit NEMO/IKK $\gamma$ . Recent X-ray crystal structures of IKK2 suggested that dimerization might be mediated by a smaller protein–protein interaction than previously thought. Here, we report that removal of a portion of the scaffold dimerization domain (SDD) of human IKK2 yields a kinase subunit that remains monomeric in solution. Expression in baculovirus-infected Sf9 insect cells and purification of this engineered monomeric human IKK2 enzyme allows for *in vitro* analysis of its substrate specificity and mechanism of activation. We find that the monomeric enzyme, which contains all of the amino-terminal kinase and ubiquitin-like domains as well as the more proximal portions of the SDD, functions *in vitro* to direct phosphorylation exclusively to residues S32 and S36 of its  $\kappa$ B $\alpha$  substrate. Thus, the NF- $\kappa$ B-inducing potential of IKK2 is preserved in the engineered monomer. Furthermore, we observe that our engineered IKK2 monomer readily autophosphorylates activation loop serines 177 and 181 *in trans*. However, when residues that were previously observed to interfere with IKK2 *trans* autophosphorylation in transfected cells are mutated within the context of the monomer, the resulting Sf9 cell expressed and purified proteins were significantly impaired in their *trans* autophosphorylation activity *in vitro*. This study further defines the determinants of substrate specificity and provides additional evidence in support of a model in which activation via *trans* autophosphorylation of activation loop serines in IKK2 requires transient assembly of higher-order oligomers.



The  $\kappa$ B kinase (IKK) complex responds to a host of proinflammatory cell stimuli by switching to a state of high catalytic activity. The prototypical IKK complex contains three subunits: IKK1/IKK $\alpha$ , IKK2/IKK $\beta$ , and NEMO/IKK $\gamma$ . IKK1 and -2 are closely related kinase domain-containing polypeptides, whereas NEMO is an obligate scaffolding subunit.<sup>1–3</sup> The essential nature of NEMO in IKK activation is illustrated by the observation that NEMO<sup>-/-</sup> MEF cells are insensitive to canonical inducers of NF- $\kappa$ B activity, including TNF- $\alpha$ , LPS, and IL-1.<sup>4</sup>

Activation of IKK1 and -2 results from the phosphorylation of two activation loop serines: S176 and S180 for IKK1 and S177 and S181 for IKK2.<sup>5</sup> Several upstream IKK kinases, including TAK1, MEKK3, and IRAK1, have been reported.<sup>6–9</sup> No single upstream kinase, however, is required for IKK activation under all conditions of signaling and across all cell types. Furthermore, several viral gene products such as HTLV Tax and KSHV v-FLIP trigger IKK activation independent of upstream signaling by directly binding to NEMO.<sup>10–13</sup> Additionally, it has been demonstrated in yeast and insect cells that overexpressed recombinant human IKK1 and -2

subunits can become activated without NEMO or any specific upstream kinase.<sup>14,15</sup> Finally, the addition of free polyubiquitin chains was shown to be sufficient to activate purified IKK1 and -2 in an *in vitro* reconstitution of IKK activation, suggesting that activation of these kinase subunits may result from *trans* autophosphorylation.<sup>16</sup>

Although active IKK recognizes and phosphorylates a number of diverse cellular substrates, including FOXO3a, p65/RelA, SNAP-23, and TSC1, its best understood function is phosphorylation of the transcription factor NF- $\kappa$ B inhibitor protein  $\kappa$ B $\alpha$  on two N-terminal serine residues, S32 and S36.<sup>17–19</sup> This signal-dependent phosphorylation of  $\kappa$ B $\alpha$  occurs in the cytoplasm and quickly leads to its ubiquitinylation and 26S proteasome-mediated degradation. The newly freed NF- $\kappa$ B then migrates to the nucleus where it elevates the expression of target genes. Mouse knockout studies clearly revealed that the IKK2 subunit is primarily responsible for this

Received: November 19, 2013

Revised: March 7, 2014

Published: March 10, 2014

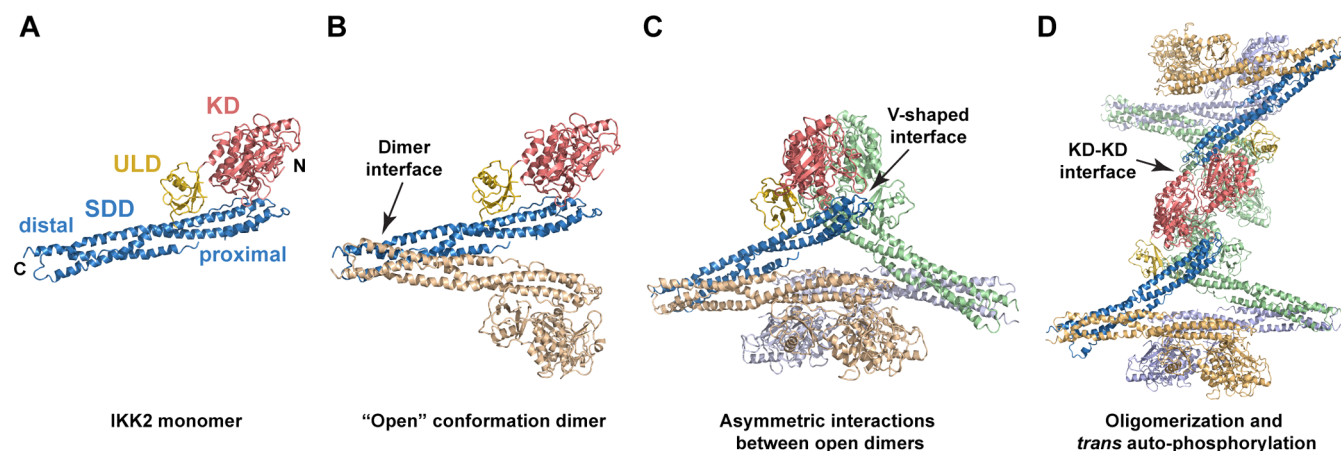


**Figure 1.** Interactions between individual IKK2 subunits. (A) As revealed by X-ray crystallography, a single IKK2 subunit contains three domains: the amino-terminal kinase domain (KD), a central ubiquitin-like domain (ULD), and a carboxy-terminal scaffold dimerization domain (SDD). The proximal portion of the SDD lies adjacent to the KD and ULD opposite the distal end. (B) Human IKK2 dimer in its open conformation, as it appears in X-ray crystal structures. Dimerization is mediated by distal portions of the SDD. (C) In their open dimeric conformation, individual IKK2 subunits can associate through an extensive V-shaped interface involving residues from the KD, ULD, and SDD. (D) Association through the V-shaped interface supports KD–KD interactions through which IKK2 can become active via activation loop *trans* autophosphorylation.

N-terminal phosphorylation of  $I\kappa B\alpha$  in response to proinflammatory NF- $\kappa B$ -inducing stimuli such as TNF- $\alpha$  or IL-1.<sup>20,21</sup>

Recent X-ray crystal structure analyses have revealed that IKK2 contains three distinct domains: an N-terminal kinase domain (KD) followed by a ubiquitin-like domain (ULD) and a C-terminal scaffold dimerization domain (SDD).<sup>22–24</sup> Dimerization of IKK2 subunits is mediated entirely by the SDD. Moreover, flexibility within this elongated  $\alpha$ -helical domain facilitates opening of the otherwise rigid IKK2 dimer (Figure 1). In their open conformation, IKK2 dimers can associate with one another to form higher-order oligomers that project their KD in a manner that supports KD–KD interactions. Introduction of mutations within surfaces that mediate these higher-order interactions disrupts IKK2 activation in transfected cells, suggesting that they facilitate IKK2 *trans* autophosphorylation.<sup>23</sup> Previous studies have also shown that IKK2 constructs that contain only the KD–ULD function *in vitro* as kinases toward their  $I\kappa B\alpha$  substrates. However, these proteins engineered to lack the entire SDD direct phosphorylation of serine and threonine residues within the C-terminus of  $I\kappa B\alpha$ , and they fail to phosphorylate S32 and S36 altogether.<sup>22,25</sup> Taken together, these observations suggest that both activation and N-terminal  $I\kappa B\alpha$  substrate specificity of IKK2 require its C-terminal SDD.

In this study, we employed structure-based design to engineer an IKK2 subunit polypeptide that is incapable of dimerization by removal of the more distal portions of its SDD. Expression and purification of this stable monomeric version enables the study of IKK2 *trans* autophosphorylation and specificity toward its  $I\kappa B\alpha$  substrate independent of dimerization. We find that the N-terminal  $I\kappa B\alpha$  substrate specificity requires KD proximal portions of the SDD but is not dependent upon IKK2 dimerization in our *in vitro* kinase assays. In contrast, disruption of dimerization severely impairs IKK2 *trans* autophosphorylation *in vitro*. Monomeric IKK2 is observed to undergo *trans* autophosphorylation at elevated concentrations only, and this forced interaction is dependent upon the surfaces that mediate oligomerization of open IKK2 dimers in the X-ray crystal structure.

## EXPERIMENTAL PROCEDURES

### IKK2 Monomer Design and Preparation of Plasmids.

Preparation of IKK2(1–420) was described previously.<sup>25</sup> IKK2<sup>mono</sup> was designed from the IKK2 X-ray crystal structure and consists of human IKK2 amino acids 11–477 joined through a Gly-Gly linker to amino acids 526–637. The IKK2(11–669)pFastBacHTb plasmid starting material was modified via a QuikChange mutagenesis protocol with the primers

IKK2 $\Delta$ (477–526)Fwd:

5'-GAATTCCATGGCTTCCATGTCTGGAGGAGA-GAACGAAGTGAACCTCCTGG-3'

IKK2 $\Delta$ (477–526)Rev:

5'-CCAGGAGTTTCACTTCGTTCTCTCCTCCAGAC-ATGGAAGCCATGGAATTC-3'

to replace IKK2 amino acids 478–525 with two glycine codons (underlined above). A stop codon (underlined below) was then introduced after residue 637 via mutagenesis using the following pair of primers

IKK2(637–stop)Fwd:

5'-GGAAGAGGTGGTGGAGCTTAATGAATTGAGAG-GATGAGAAGACTGTTGTCCG-3'

IKK2(637–stop)Rev:

5'-CGGACAACAGTCTTCTCATCCTCTCAATTC-ATTAAGCTCACCACTCTTCC-3'

For mutagenesis of the activation loop serines 177 and 181 to phosphomimetic glutamic acid residues, the following primers were used (mutations underlined)

IKK2EE Fwd:

5'-GAGCTGGATCAGGGCGAGCTTTGCACAGAATT-CGTGGGGACCC-3'

IKK2EE Rev:

5'-GGGTCCCCACGAATTCGTGTGCAAAGCTCGC-CCTGATCCAGCTC-3'

Mutations were also introduced to change serines 177 and 181 to alanines to generate an inactivatable IKK2 protein as well as to mutate the aspartic acid catalytic base residue 145 to asparagine to create a kinase dead variant. The following primers were used (mutations are underlined)

IKK2AA Fwd:

5'-GAGCTGGATCAGGGCGCTCTT-TGCACAGCATTCTGGGGACCC-3'

IKK2AA Rev:

5'-GGGTCCCACGAATGCTGTGCAAAGAGCGC-CCTGATCCAGCTC-3'

IKK2D145N Fwd:

5'-CAGAATCATCCATCGGAATCTAAAGCCAGA-AAACATC-3'

IKK2D145N Rev:

5'-GATGTTTCTGGCTTTAGATTCCGATGGATG-ATTCTG-3'

Additionally, on the basis of the V-shaped and KD–KD interface mutants that exhibited the most defective IKK2 activation in transfected HEK293T cells,<sup>23</sup> the following primers were used to introduce these mutations in the context of IKK2<sup>mono</sup> (mutations are underlined)

IKK2I413A/L414A Fwd:

5'-CAACCTGAAAGTGTGCTGCTGCTCA-AGAGCCCAAGAGGAATCTC-3'

IKK2I413A/L414A Rev:

5'-GAGATTCCTCTTGGGCTCTTGAGCAGCAC-AGCTGACACTTTCAGTTG-3'

IKK2 V229A/H232A Fwd:

5'-CCCCAACTGGCAGCCCGCGCAGTGGGCTTC-AAAAGTGCAGCAGAAG-3'

IKK2 V229A/H232A Rev:

5'-CTTCTGCCGCACTTTGAAGCCCACTGCGCGGG-CTGCCAGTTGGGG-3'

**Preparation of Recombinant Baculoviruses.** Production and titering of recombinant baculoviruses were carried out using a modified version of the standard Bac-to-Bac protocol (Invitrogen). This has been detailed previously.<sup>25</sup>

**Protein Expression and Purification.** Sf9 suspension cultures at a cell density of  $2 \times 10^6$  cells/mL were infected with recombinant baculovirus encoding IKK2<sup>mono</sup> for 48–72 h at 26 °C. Cells from 1 L cultures were harvested by centrifugation and lysed in 100 mL of lysis buffer (25 mM Tris-HCl, pH 8.0, 200 mM NaCl, 10 mM imidazole, 10% w/v glycerol, 5 mM  $\beta$ -mercaptoethanol, and 1 $\times$  Sigma protease inhibitor cocktail) by two 30 s cycles of sonication at a duty cycle of 40% and a power output setting of 4 using a Branson Sonifier 450. One-hundred microliters of 200 mM PMSF was added immediately before each cycle. The lysate was clarified by centrifugation at 14 000 rpm (Sorvall; SS-34 rotor) for 45 min at 4 °C and passed through a 0.8  $\mu$ m syringe filter. Pre-equilibrated Ni Sepharose Fast Flow resin (GE Life Sciences) was added at a ratio of 1 mL of resin slurry/liter of lysed cell culture. The mixture was allowed to incubate at 4 °C on a rotator for 1.5 h. The Ni resin was then pelleted at 1000 rpm for 10 min in a swinging bucket rotor centrifuge. Supernatant was carefully decanted, and the protein-bound resin was resuspended with an equal volume of lysis buffer and allowed to incubate at 4 °C on a rotator for an additional 15 min. The Ni resin was pelleted again, supernatant was decanted (wash 1), and an equal volume of wash buffer (lysis buffer containing 500 mM NaCl and 30 mM imidazole) was added. This Ni resin/wash buffer mixture was allowed to incubate on a rotator for an additional 15 min, at which point the resin was pelleted and the wash buffer was decanted. The washed resin was then transferred to a 5 mL gravity column casing, and the resin was allowed to settle. Elution buffer (lysis buffer containing 250 mM imidazole) was added, and eluted fractions were collected. Peak fractions containing IKK2 were pooled and loaded onto a preparative Superdex200 16/60 size-

exclusion column connected to an ÄKTA Basic chromatography system (GE Life Sciences) equilibrated with 20 mM Tris-HCl, pH 8.0, 150 mM NaCl, 5 mM DTT, and 5–10% glycerol. Peak fractions were concentrated by centrifugation using a 30 kDa cutoff membrane concentrator unit to 5–10 mg/mL. Protein concentration was determined by Bio-Rad Protein Assay, and protein was flash frozen in liquid N<sub>2</sub> and stored at –80 °C.

**Circular Dichroism Spectroscopy.** IKK2EE(11–669) homodimers and IKK2EE<sup>mono</sup> were dialyzed separately with Slide-a-Lyzers (Pierce; 10 000 MWCO) into 20 mM sodium phosphate buffer (pH 7.4), filtered through 0.2  $\mu$ m syringe filters (Millipore) and then further diluted to 0.6 mg/mL. Far-UV CD spectra were collected for 250  $\mu$ L samples in a nitrogen-purged 0.1 mm quartz cuvette on an Aviv-420 spectropolarimeter operated at 1.0 nm bandwidth in 1 nm steps from 260 to 185 nm. Two spectra were averaged for each final readout. For secondary-structure assignment, the mdeg data files were converted into molar ellipticity per residue and submitted through DichroWeb for analysis by SELCON3 prediction software using reference file no. 7.<sup>26–28</sup>

**Size-Exclusion Chromatography–Multiangle Laser Light Scattering (SEC–MALLS).** Twenty microliters of purified IKK2<sup>mono</sup> was injected into a pre-equilibrated (20 mM Tris-HCl, pH 8, 150 mM NaCl, and 5% w/v glycerol) Zenix SEC-300, 7.8  $\times$  300 mm column (Sepax Technologies, Inc.) at 1 mL/min. Elution of the protein was monitored by UV–vis (Shimadzu SPD-10A VP) and refractive index (Hitachi L-2490) detectors. Light scattering was monitored with a Dawn-Helios multiangle detector (Wyatt technology). Astra VI software (Wyatt Technology) was used to analyze light scattering data. Figures were prepared in Excel.

**In Vitro Kinase Assay.** *In vitro* kinase assays were conducted in 20  $\mu$ L reactions using purified IKK2 (20–600 ng) with or without purified substrate (2  $\mu$ g) or kinase dead D145N IKK2 (0.5–1  $\mu$ g) and a reaction buffer consisting of 20 mM Tris-HCl, pH 7.5, 15 mM MgCl<sub>2</sub>, 50 mM KCl, 1 mM DTT, 1 mM Na<sub>3</sub>VO<sub>4</sub>, 20 mM  $\beta$ -glycerophosphate, 10 mM NaF, and 20  $\mu$ M ATP. To these reactions, was added 0.5  $\mu$ Ci of  $\gamma$ -<sup>32</sup>P ATP (PerkinElmer), and the reactions were mixed and incubated at room temperature for the indicated time points up to 1 h. After incubation, 7  $\mu$ L of Laemmli buffer was added to quench the reaction, and 10  $\mu$ L of the mixture was loaded and resolved on a 10% SDS PAGE gel. The gel was subsequently dried on no. 3 Whatman filter paper and then exposed to autoradiography film for approximately 12–16 h prior to developing.

**Western Blot.** Standard semidry western blotting protocols were employed. All samples were separated by 10% SDS-PAGE before being transferred to nitrocellulose. A 0.2% w/v I-Block solution (Applied Biosystems) was used as a blocking agent. Monoclonal mouse penta-His antibody (Qiagen) was diluted 1:4000 and used for primary detection of His-tagged proteins. Rabbit monoclonal 16A6 (Cell Signaling Technology) was employed at a 1:1500 dilution to monitor IKK2 activation loop phosphorylation status.

## RESULTS

**Design and Engineering of an IKK2 Monomer.** Comparative analysis of the *Xenopus* and human IKK2 X-ray crystal structures revealed that individual IKK2 dimers exhibit various degrees of opening. The *Xenopus* IKK2 structure adopts a relatively closed conformation in which two subunits of the

dimer associate through the entire length of the SDD.<sup>22</sup> A closed conformation is also observed for the IKK-related TBK1 enzyme. In TBK1, however, the KD from each protomer also contacts the SDD of its dimer-forming partner, resulting in an even more compact dimer.<sup>29,30</sup> Two recently published crystal structures of human IKK2 reveal that the dimer can adopt significantly more open conformations in which the KD–ULD swing away from one another, suggesting that dimerization is mediated entirely through portions of the SDD that are distal to the KD.<sup>23,24</sup>

The SDD of IKK2 and TBK1 is effectively an elongated three-helix bundle in which two parallel  $\alpha$ -helices of roughly 115 Å in length ( $\alpha 2s$  and  $\alpha 6s$ ) are connected by an equally long antiparallel stretch containing three shorter helices ( $\alpha 3s$ – $\alpha 5s$ ). The open conformations observed for the human IKK2 models suggest that the SDD mediates flexibility. Indeed, superposition of *Xenopus* and human IKK2 models that display differing degrees of openness reveals that the structures are all roughly equivalent within either the KD–ULD–proximal SDD portions or the distal SDD but differ to a significantly greater degree for the entire subunits (Table 1). For example,

**Table 1. Average rmsd for IKK2 Subunits<sup>a</sup>**

| entire IKK2 subunit (all amino acids)             |             |             |                   |
|---|-------------|-------------|-------------------|
|   | 3QA8        | 4E3C        | 4KIK              |
| 3QA8  | 1.30 ± 0.29 | 2.67 ± 0.22 | 3.15 ± 0.35       |
| 4E3C  |             | 1.17 ± 0.18 | 2.08 ± 0.20       |
| 4KIK  |             |             | 1.54 <sup>b</sup> |
| IKK2 monomer (amino acids 1–477 and 526–637)      |             |             |                   |
|   | 3QA8        | 4E3C        | 4KIK              |
| 3QA8  | 0.44 ± 0.08 | 1.70 ± 0.08 | 2.28 ± 0.09       |
| 4E3C  |             | 0.68 ± 0.10 | 1.74 ± 0.15       |
| 4KIK  |             |             | 1.06 <sup>b</sup> |
| IKK2 distal SDD (amino acids 477–526 and 638–666) |             |             |                   |
|   | 3QA8        | 4E3C        | 4KIK              |
| 3QA8 <sup>a</sup>                                 | 0.48 ± 0.13 | 1.64 ± 0.08 | 1.32 ± 0.08       |
| 4E3C  |             | 1.13 ± 0.27 | 1.66 ± 0.15       |
| 4KIK  |             |             | 0.21 <sup>b</sup> |

<sup>a</sup>Units are in angstroms. Values are calculated as the average of the rmsd values for C $\alpha$  positions after superposition of individual IKK2 subunit models from three published IKK2 X-ray crystal structures: *Xenopus laevis* (3QA8) and human (4E3C and 4KIK).<sup>22–24</sup> 95% confidence level. <sup>b</sup>Only one measurement available (chain A vs chain B).

overlaying the distal portion of the SDD (a discontinuous segment consisting of amino acids 477–526 and 638–666) from each of the *Xenopus* IKK2 subunits upon the same portion of the human IKK2 protomers (PDB code 4E3C) results in an average root-mean-squared deviation (rmsd) for C $\alpha$  atoms of 1.64 Å. Superposition of the remaining portions of the same IKK2 subunits (amino acids 1–477 and 526–637) yields an average rmsd of 1.70 Å. However, when full IKK2 subunits are superimposed, the average rmsd for C $\alpha$  atoms measures 2.67 Å. This suggests that the structural changes that lead to the different degrees to which IKK2 adopts its open conformation are focused at a position around Gly525 between SDD helices  $\alpha 3s$  and  $\alpha 4s$ . It also suggests that, other than this hinge point, the remaining portions of the kinase are relatively rigid.

We tested this hypothesis by designing, expressing, and purifying an IKK2 construct that lacks its distal SDD region

(Figure 2). The distal portion of the SDD was removed by replacing residues 477–526 (from  $\alpha 2s$  and  $\alpha 3s$ ) with a Gly-Gly linker and inserting a stop codon after residue 637 in  $\alpha 6s$  (Figure 2A,B). Recombinant baculoviruses encoding for this protein were generated and used to infect Sf9 insect cell suspension cultures. Purification by Ni affinity and size-exclusion chromatography yielded a pure protein, as judged by Coomassie-stained SDS PAGE (Figure 2C). Its elution volume on size-exclusion chromatography is consistent with the deletion protein behaving as a monomer in solution (Figure 2D). Therefore, we have dubbed this engineered enzyme IKK2<sup>mono</sup>.

**Circular Dichroism Spectroscopy of IKK2<sup>mono</sup>.** To confirm that deletion of the residues in question does not severely alter protein secondary structure, we carried out far-UV circular dichroism (CD) spectroscopy on IKK2EE(11–669) dimers and IKK2EE<sup>mono</sup> proteins in solution. Both spectra exhibit strong troughs at 208 and 222 nm that are characteristic of proteins with significant  $\alpha$ -helical character (Figure 3). Analysis of the spectra using DichroWeb estimates the degree of  $\alpha$ -helical content in IKK2EE(11–669) to be 45%.<sup>26</sup> This agrees remarkably well with values calculated from Ramachandran angles of the refined crystallographic model that suggest the protein is 46%  $\alpha$ -helical. CD recognizes IKK2EE<sup>mono</sup> as 35%  $\alpha$ -helical. Although this is slightly lower than the 43%  $\alpha$ -helical content calculated from a theoretical model created from simply removing residues from the IKK2EE(11–669) X-ray crystal structure, it is significantly higher than the 18%  $\alpha$ -helix contributed by the KD alone. Moreover, the difference in measured  $\alpha$ -helicity of IKK2 monomer and dimer is accounted for primarily by an increase in turns in the monomer, the  $\beta$ -sheet and disordered portions calculated from the CD spectra remain unchanged. Therefore, we conclude that the truncated SDD of our IKK2<sup>mono</sup> proteins remains predominantly  $\alpha$ -helical after removal of three  $\alpha$ -helical passes that mediate dimerization.

**IKK2<sup>mono</sup> Retains Specificity for N-Terminal Serine Phosphorylation Sites of I $\kappa$ B $\alpha$ .** It was previously demonstrated that C-terminal truncations of IKK2 that eliminate the SDD entirely result in a kinase defective in its ability to recognize S32 and S36 of I $\kappa$ B $\alpha$  *in vitro*. These shortened versions instead direct phosphorylation toward serine and threonine residues contained within the I $\kappa$ B $\alpha$  C-terminal PEST-like region.<sup>22,25</sup> The *Xenopus* and human IKK2 X-ray crystal structures reveal that the KD, ULD, and SDD participate in extensive interdomain interactions. The introduction of point mutations to destabilize IKK2 domain–domain interfaces was shown to measurably reduce the activity of full-length IKK2 toward I $\kappa$ B $\alpha$  *in vitro*.<sup>23</sup> IKK2<sup>mono</sup> maintains each of these critical interdomain interactions.

Four different versions of the human IKK2 subunit expressed and purified from baculovirus infected Sf9 insect cell suspensions were incubated independently with five different purified I $\kappa$ B $\alpha$  substrate proteins and Mg/ $\gamma$ -<sup>32</sup>P-ATP to observe the specificity of I $\kappa$ B $\alpha$  phosphorylation *in vitro* (Figure 4). Both the full-length IKK2 and the IKK2(11–669) protein that was previously employed for X-ray crystal structure determination phosphorylated I $\kappa$ B $\alpha$  exclusively on S32 and S36 (Figure 4; lanes 1–11). Both of these enzymes contained the S177E and S181E activation loop mutations that render the enzyme constitutively active. To test whether this pair of activation loop Glu mutations alone is sufficient to direct substrate specificity toward the N-terminal region of I $\kappa$ B $\alpha$ , we next prepared a

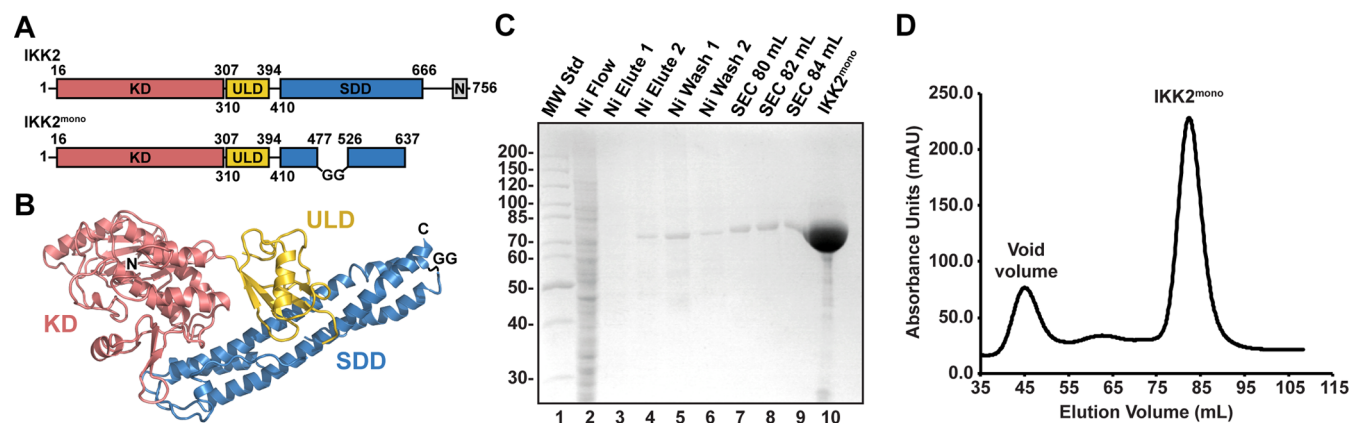


**Figure 2.** Engineered monomeric IKK2 (IKK2<sup>mono</sup>). (A) Schematic diagram of the domain organization of the IKK2 subunit (above) and IKK2<sup>mono</sup> (below). Coloring and abbreviations are shown as in Figure 1. Numbers correspond to the domain borders in the human IKK2 subunit, and GG refers to the diglycine linker joining SDD helices  $\alpha 2s$  and  $\alpha 4s$ . (B) Ribbon diagram model of the expected IKK2<sup>mono</sup> structure on the basis of the X-ray crystal structure of human IKK2EE(11–669). (C) Coomassie-stained 10% SDS-PAGE analysis monitoring IKK2<sup>mono</sup> purification by Ni affinity (lanes 2–6) and size-exclusion (lanes 7–9) chromatography and the final concentrated protein (lane 10). (D) Representative chromatogram of size-exclusion chromatography on IKK2<sup>mono</sup>.

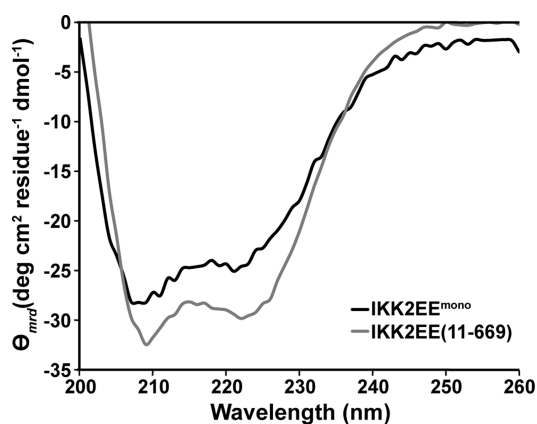


**Figure 3.** Circular dichroism spectroscopy of purified IKK2 proteins. The mean residue molar ellipticity for IKK2EE<sup>mono</sup> (black line) and IKK2EE(11–669) (gray line) is plotted as a function of wavelength. Both samples show strong  $\alpha$ -helical signals, with the monomer showing a slight decrease, as predicted because of the removal of three largely  $\alpha$ -helical passes at the dimer interface.

human IKK2(1–420) that lacks its entire C-terminal SDD but still bears the S177E and S181E mutations (Figure 4; lanes 12–16). Just as we observed previously when assaying a similar protein construct with an activation loop of native (S177 and S181) sequence, the enzyme lacking its SDD functioned as an efficient catalyst to phosphorylate C-terminal residues of I $\kappa$ B $\alpha$  and completely failed to recognize I $\kappa$ B $\alpha$  substrate residues S32 and S36.<sup>25</sup>

Our newly engineered IKK2<sup>mono</sup> displayed identical specificity *in vitro* as the full-length kinase. That is, it phosphorylated I $\kappa$ B $\alpha$  exclusively at S32 and S36 (Figure 4; lanes 17–21). This observation confirms that portions of the SDD proximal to and in contact with the KD–ULD are required for the phosphorylation event that results in induction of NF- $\kappa$ B transcriptional activity in response to proinflammatory signaling in mammalian cells.

**Solution Behavior of Engineered IKK2 Monomers.** It has been shown previously that IKK2 dimerization is required for its efficient activation.<sup>15</sup> For example, mutation of residues that mediate dimer contacts within the distal portion of the

SDD yields an IKK2 enzyme that exhibits significantly lower *in vitro* catalytic activity after purification from baculovirus-infected insect cells or transfected human cells.<sup>22,23</sup> The level of phosphorylation activity by IKK2<sup>mono</sup> in our *in vitro* assay was reasonably high, which is interesting considering that its activation loop serines were not mutated to constitutively activating glutamic acid residues. This suggests that, even though the IKK2<sup>mono</sup> protein purifies as a monomer in solution, it might be capable of becoming activated by trans autophosphorylation *in vitro*.

Our previous structure-based biochemical investigations into the mechanism of IKK2 activation led to the conclusion that low-affinity interactions between IKK2 dimers through their so-called V-shaped interface stabilizes the kinase domains in a conformation that supports KD–KD interactions and promotes activation by trans autophosphorylation (Figure 1). Under this model, the principal activating signal required immediately upstream of IKK2 activation is a simple increase in the effective concentration of IKK2. This is likely a function carried out *in vivo* by the scaffolding protein NEMO via a process that depends upon its interaction with polyubiquitin chains.<sup>31</sup>

To observe its propensity for self-association in solution, we next determined the shape-independent molecular weight of IKK2<sup>mono</sup> at different concentrations by SEC–MALLS. We first compared IKK2<sup>mono</sup> directly with full-length IKK2 and IKK2EE(11–669), the construct that was previously employed successfully for X-ray crystallography. As suggested by size-exclusion chromatography during purification, SEC–MALLS clearly reveals that IKK2<sup>mono</sup> exists exclusively as a monomer in solution, whereas full-length IKK2 and IKK2EE(11–669) are dimers (Figure 5A). We next analyzed IKK2<sup>mono</sup> at increasing concentrations and observed that it remains a monomer even at a concentration of 187  $\mu$ M (Figure 5B). These observations further support the hypothesis that IKK2 dimerization is mediated entirely by the distal portion of the SDD. Furthermore, it suggests that other additional IKK2 oligomeric binding events, such as association through the V-shaped interface that was demonstrated to promote trans autophosphorylation, are of considerably low affinity.

**Activation Loop Phosphorylation by IKK2 Monomers.** We previously reported that when IKK2 V-shaped interface

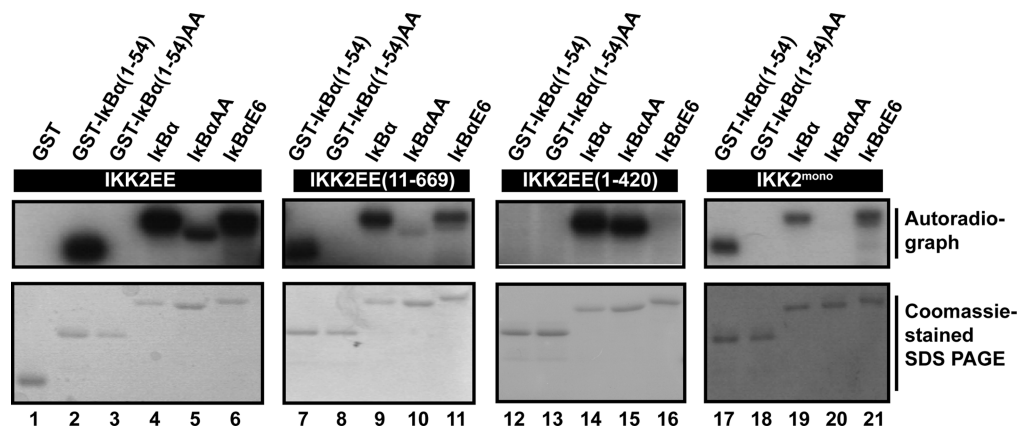


**Figure 4.** IKK2<sup>mono</sup> is specific for IκBα residues S32 and S36. *In vitro* kinase assays were performed with full-length human IKK2EE (lanes 1–6), IKK2EE(11–669) (lanes 7–11), IKK2EE(1–420) (lanes 12–16), and IKK2<sup>mono</sup> (lanes 17–21) against both native sequence or S32A/S36A (AA) GST–IκBα(1–54) substrates as well as native, S32A/S36A, or C-terminal S283E/S288E/T291E/S293E/T296E/T299E (E6) mutant full-length IκBα substrates. Two-hundred nanograms of kinase was used in each assay except for the IKK2EE(1–420) reactions, which contained 400 ng of enzyme each. Substrate specificity is revealed by autoradiography (top panels) and Coomassie-stained SDS-PAGE substrate loading controls (bottom panels).

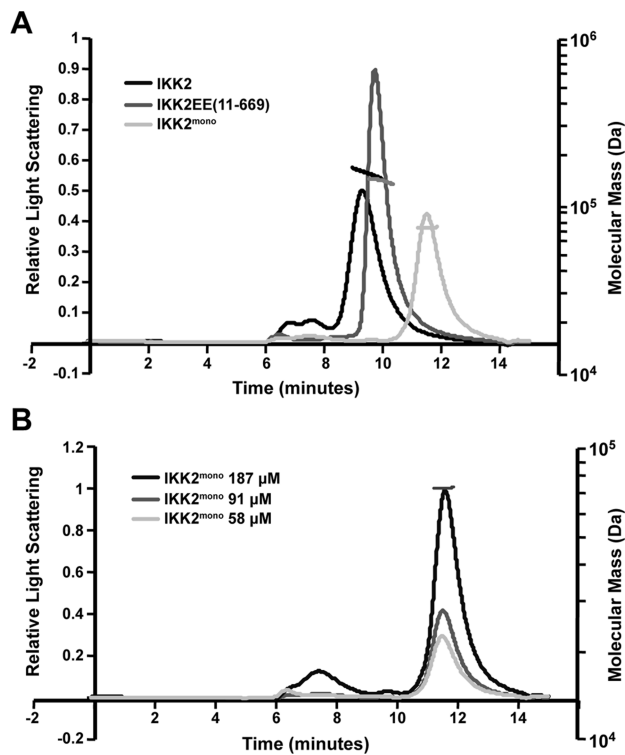


**Figure 5.** IKK2 oligomerization state in solution. (A) Full-length IKK2 (black line) and IKK2EE(11–669) (dark gray) are both dimers in solution, as revealed by multiangle laser light scattering following size-exclusion chromatography (SEC–MALLS). IKK2<sup>mono</sup> (light gray) is a monomer. (B) Increasing the IKK2<sup>mono</sup> concentration to as high as 187 μM does not significantly affect its profile as a monomer in solution.

residues I413 and L414 were both mutated to alanine and then expressed by transfection in HEK293 cells the resulting kinase was seriously impaired in its ability to become active through activation loop phosphorylation. Similarly, double mutation of residues V229 and H232, which are positioned to mediate KD–KD interactions during trans autophosphorylation, to alanine exhibited an even more severe defect. In the case of both mutants, versions in which activation loop serines 177 and

181 were also mutated to glutamic acid displayed *in vitro* kinase activity equal to constitutively active versions of the wild-type IKK2 sequence.<sup>23</sup>

Oligomerization of two IKK2 subunits through their V-shaped interface involves surface residues from the KD, ULD, and a proximal portion of the SDD but does not necessarily require dimerization through the distal end of the SDD. Therefore, as part of our effort to characterize oligomerization-dependent trans autophosphorylation *in vitro*, we employed our Sf9 insect cell expression capabilities to overexpress and purify mutant versions of IKK2<sup>mono</sup> in which key amino acid residues were mutated. Both the IKK2<sup>mono</sup> I413A/L414A and V229A/H232A mutant proteins express to similar levels and purify as monomers, suggesting that they are folded similarly to the IKK2<sup>mono</sup> wild-type sequence.

It has been shown previously that overexpression of IKK2 absent NEMO in Sf9 and yeast cell cultures yields active IKK2.<sup>14,15,23</sup> In agreement with this observation, we detect phosphorylation of activation loop serine 181 by immunoblot of overexpressed and purified IKK2 prior to the addition of ATP (Figure 6A; lanes 1–4). This zero time point S181 phosphorylation is also observed for the full-length IKK2 bearing the I413A/L414A V-shaped interface mutations, suggesting that disruption of this interface is not sufficient to impede activation loop phosphorylation when IKK2 is overexpressed in Sf9 insect cells (Figure 6A; lanes 5–8). Interestingly, S181 phosphorylation could also be detected in the engineered monomeric IKK2<sup>mono</sup> (Figure 6A; lanes 9–12). This indicates that dimerization is not an absolute requirement for IKK2 trans autophosphorylation. However, when both the distal SDD dimerization region and V-shaped interface are compromised, we failed to observe activation loop phosphorylation either before or after incubation with ATP (Figure 6A; lanes 12–16). This observation suggests that both dimerization through the distal SDD and oligomerization via the V-shaped interface contribute to spontaneous kinase activation when IKK2 is expressed in insect cells.

We have hypothesized that the observed S181 phosphorylation is a consequence of IKK2 trans autophosphorylation because of the relatively high kinase concentrations obtained upon Sf9 cell infection. To test if IKK2<sup>mono</sup> is, in fact, capable of

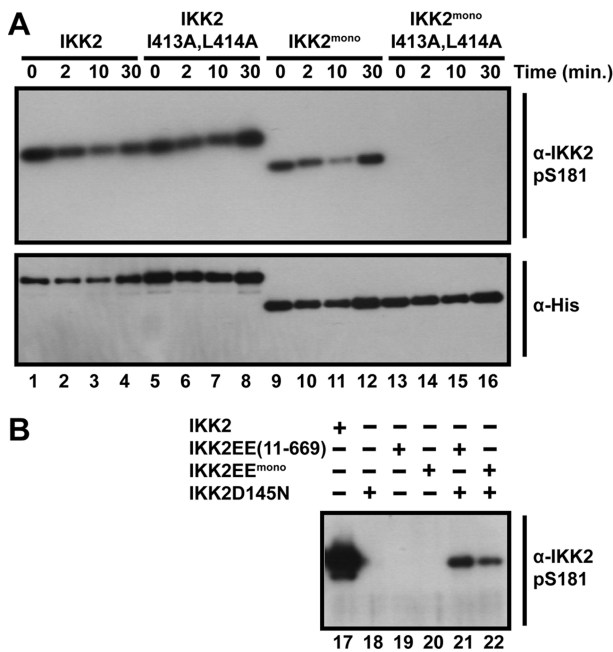


**Figure 6.** Activation loop phosphorylation activity of IKK2 dimers and monomers. (A) Western blot analysis with an anti-phospho-S181 antibody on recombinant human IKK2 proteins purified from baculovirus-infected Sf9 insect cells before and after treatment with Mg/ATP (top). Only IKK2<sup>mono</sup> in which V-shaped interface residues I413 and L414 are both mutated to alanine fails to be recognized by the antibody (lanes 13–16). Western with anti-His antibody confirms the level of protein in each reaction (bottom). (B) Catalytically inactive version of full-length IKK2 in which catalytic base D145 is mutated to Asn permits direct detection of activation loop trans autophosphorylation. Western blot reveals that constitutively active versions of both dimeric and monomeric IKK2 bearing the S177E/S181E mutations (EE) phosphorylate the IKK2D145N substrate *in vitro* (lanes 21 and 22).

catalyzing phosphorylation of IKK2 activation loop in trans, serines 177 and 181 of the IKK2<sup>mono</sup> were mutated to glutamic acid residues to produce a constitutively active version (referred to as IKK2EE<sup>mono</sup>). *In vitro* kinase reactions were then carried out using a catalytically inactive version of the full-length IKK2, in which the catalytic D145 residue was mutated to asparagine (IKK2D145N), as substrate and probed by immunoblot for S181 phosphorylation (Figure 6B). The crystallized IKK2EE(11–669) and, albeit to a lesser extent, the IKK2EE<sup>mono</sup> enzymes both were found to be capable of phosphorylating S181 of full-length IKK2D145N.

**Activation of IκB Kinase Activity in Monomeric IKK2.**

We next assessed whether oligomerization-dependent trans autophosphorylation was sufficient to activate IKK2 independent of its ability to form dimers. Relative to the engineered IKK2<sup>mono</sup> enzyme of native sequence, purified IKK2<sup>mono</sup> enzymes that harbored mutations at their V-shaped (I413A/L414A) and KD–KD (V229A/H232A) interface surfaces were severely compromised in their ability to phosphorylate the GST–IκBα(1–54) substrate in  $\gamma$ -<sup>32</sup>P-ATP *in vitro* kinase assays (Figure 7A; lanes 1–3). The introduction of activation loop S177E/S181E mutations against these IKK2<sup>mono</sup> interfacial mutants resulted in significant recovery of *in vitro* catalytic activity toward GST–IκBα(1–54) (Figure 7A; lanes 4–5). This suggests that the incapability of the IKK2<sup>mono</sup> I413A/L414A and V229A/H232A mutants to function as IκB kinases

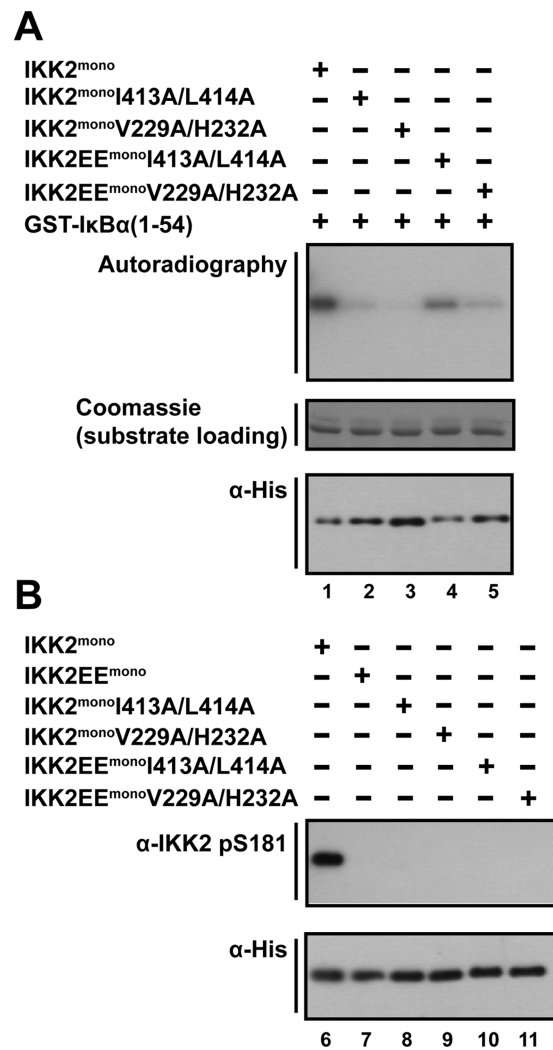


**Figure 7.** Role of trans autophosphorylation in activation of IKK2<sup>mono</sup>. (A) Autoradiography of *in vitro* kinase assays with GST–IκBα(1–54) as substrate and various versions of IKK2<sup>mono</sup> as enzymes (top). Both mutation of the V-shaped (I413A/L414A) and KD–KD (V229A/H232A) interfaces yields IKK2<sup>mono</sup> proteins that almost completely lack kinase activity toward GST–IκBα(1–54) substrate (lanes 1–3). Conversion of both activation loop residues S177 and S181 to phosphomimetic glutamic acids (EE) results in IKK2<sup>mono</sup> enzymes that display significantly higher kinase activity. Coomassie-stained SDS PAGE substrate and anti-His western blot enzyme loading controls are shown below. (B) Western blot with anti-phospho-S181 antibody reveals that only native sequence IKK2<sup>mono</sup> is capable of activation loop autophosphorylation (compare lanes 6, 8, and 9; above). Anti-His western blot loading control (bottom).

results from their inability to support activation via trans autophosphorylation.

To test this hypothesis further, we next used immunodetection to probe the phosphorylation state of activation loop S181 in native sequence and interfacial mutant IKK2<sup>mono</sup> enzymes after incubation with Mg and ATP. Only IKK2<sup>mono</sup> containing the native sequence activation segment (S177 and S181) could be recognized by antibodies specific for IKK2 phosphoserine-181 (Figure 7B). As controls, we also tested the IKK2<sup>mono</sup> proteins that contained activating S177E/S181E activation loop mutations. As expected, these proteins failed to react with the anti-IKK2 pSer181 antibody.

**Oligomerization-Dependent Trans Autophosphorylation of IKK2.** Our *in vitro* experiments with the engineered monomeric IKK2 enzyme reveal that its ability to become activated via trans autophosphorylation on its activation loop serines is impaired. Moreover, although after activation it retains its specificity for S32 and S36 of IκBα, IKK2<sup>mono</sup> displays measurably lower catalytic activity toward its namesake substrate. These observations support many previously reported studies that have concluded that IKK2 dimerization plays an integral role in its activation and consequently its ability to function as an IκB kinase.<sup>15,22,32</sup> However, our observations also suggest that IKK2<sup>mono</sup> harbors all of the residues necessary to mediate activation and substrate specificity.

To test the hypothesis that the V-shaped and KD–KD oligomerization interfaces observed in our X-ray crystal structure are sufficient to support IKK2 activation via trans autophosphorylation, we performed a time-course experiment in which the ability of various IKK2 dimers and monomers to phosphorylate S181 of the inactive IKK2D145N mutant was monitored by western blot (Figure 8). All of the active kinases in this experiment harbored the activating S177E/S181E mutations. At a concentration of 150 nM enzyme/300nM

substrate, we observed that the dimeric IKK2EE(11–669) could turn over product, whereas various IKK2<sup>mono</sup> mutant proteins did not display activity (Figure 8; lanes 1–8). After increasing the enzyme concentration to 300 nM, however, significant phosphorylation of the inactive IKK2D145N substrate could be detected (Figure 8; lanes 9–16). The IKK2<sup>mono</sup> I413A/L414A mutant that harbors mutations targeting the V-shaped interface showed significantly less activity, although activity could be detected at an enzyme concentration of 450 nM (Figure 8; lanes 17–24). Mutation of the KD–KD residues V229 and H232 yielded an IKK2<sup>mono</sup> enzyme that failed to produce detectable amounts of S181 phosphorylation at all of the concentrations tested. This experiment supports the hypothesis that activation loop phosphorylation in trans is mediated by IKK2 oligomerization interfaces in addition to dimerization.

■ DISCUSSION

Protein kinases share a conserved domain structure and catalytic mechanism for phosphoryl transfer from ATP to protein substrate.<sup>33</sup> What distinguishes one protein kinase from another, therefore, is their ability to act upon select substrates and their mechanisms for regulating catalytic activity.<sup>34,35</sup> IKK is unique on both fronts. IKK was first cloned biochemically because it was the only kinase activity detected in TNF-α-treated HeLa cells that could specifically phosphorylate serines 32 and 36 of the NF-κB inhibitor protein IκBα.<sup>17,18,36</sup> Despite numerous studies aimed at uncovering a basis for this substrate specificity, it is still not perfectly clear how IKK only facilitates this chemistry. The field of regulation of IKK activity has received significantly more attention, with literally thousands of published studies. These efforts have led to many seminal discoveries, including the fundamental role of ubiquitin as an activating component of cell signaling complexes.<sup>37,38</sup> Nevertheless, basic questions surrounding the regulatory control of IKK persist. Among these, does IKK activation require any upstream kinase? How does interaction with polyubiquitin promote kinase activity? Are the extremely rapid kinetics of IKK activation observed in cells suggestive of a relatively simple activation mechanism?

We have previously shown that a version of IKK2 containing only the amino-terminal KD and ULD recognizes and phosphorylates its IκBα substrate *in vitro*. However, this IKK2(1–420) fragment directs its activity toward serine and threonine residues contained within the C-terminal PEST-like region of IκBα and fails to recognize S32 and S36 altogether.<sup>25</sup> This surprising observation could be explained by one of three different factors. First, it is possible that the activation loop of IKK2(1–420) fails to become phosphorylated in the absence of its C-terminal SDD, and in its unphosphorylated state, the kinase displays altered specificity toward IκBα. A second possibility arises from the fact that the shortened IKK2(1–420) is a monomer in solution. Therefore, it is possible that dimerization through the SDD somehow directs specificity toward S32 and S36 of IκBα. The third possibility is that elements from the SDD itself are directly involved in docking and/or presenting the IκBα substrate such that S32 and S36 can be targeted. We tested a version of the IKK2(1–420) construct in which activation loop residues S177 and S181 are mutated to phosphomimetic glutamic acid residues and found that this enzyme displays the same specificity toward the C-terminal residues of IκBα, effectively disproving the hypothesis

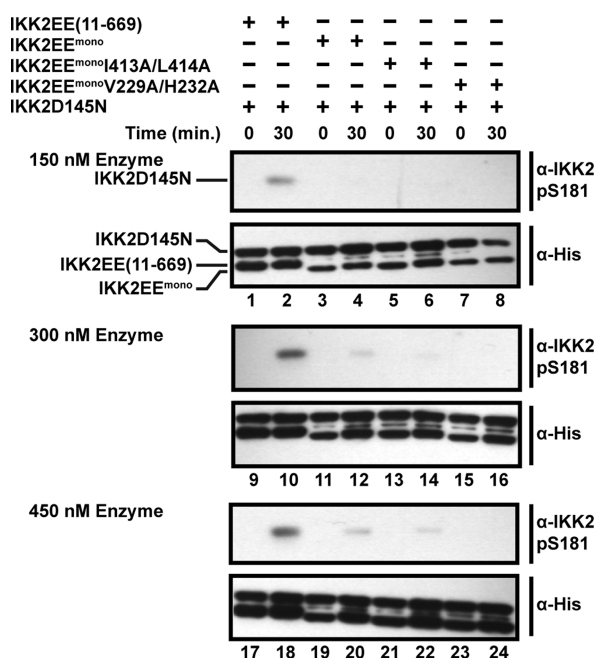


**Figure 8.** Activation loop trans autophosphorylation by mutant IKK2<sup>mono</sup> enzymes can be partially recovered at high concentration. The activation loop phosphorylation state of the inactive IKK2D145N mutant is monitored via western blot with anti-phospho-S181 antibody. Enzyme concentrations are given; IKK2D145N was 300 nM in each reaction. Dimeric and constitutively active IKK2EE(11–669) readily phosphorylates activation loop S181 (lanes 1 and 2). IKK2EE<sup>mono</sup> also phosphorylates the inactive IKK2D145N substrate, although a higher concentration of enzyme is required to observe comparable levels of phosphorylation (compare lanes 3 and 4, 11 and 12, and 19 and 20). Mutation of V-shaped interface residues I413 and L414 to alanine yields an IKK2EE<sup>mono</sup> enzyme that is even more defective in trans autophosphorylation of IKK2D145N *in vitro*. Mutation of KD–KD interaction residues V229 and H232 to alanine yields an IKK2EE<sup>mono</sup> enzyme that fails to trans autophosphorylate even when provided in molar excess to the IKK2D145N substrate protein.



that activation loop phosphorylation status dictates specificity (Figure 4; lanes 17–21).

Recent success in X-ray crystallography of nearly full-length IKK2 homodimers has revealed the domain organization and arrangement of individual subunits in the functioning dimer.<sup>22–24</sup> The observation that these IKK2 homodimers can exhibit varying degrees of opening has allowed identification of the dimerization interface within the portion of the SDD distal to the KD–ULD. In the present study, we have engineered a minimal IKK2 that lacks the distal portion of the SDD and consequently purifies as a stable monomer. This IKK<sup>mono</sup> protein displays ideal solution behavior. Furthermore, kinase assays reveal that IKK<sup>mono</sup> faithfully reconstitutes S32 and S36 phosphorylation of I $\kappa$ B $\alpha$  *in vitro*. We conclude that elements within the proximal portion of the SDD are necessary for directing specificity of IKK2 toward I $\kappa$ B $\alpha$  S32 and S36, independent of the dimerization status of the enzyme. The IKK2 X-ray crystal structures reveal that this portion of the SDD contacts both the KD and ULD, and mutations introduced to disrupt these interdomain interactions were previously shown to interfere with catalytic activity. It is likely that the proximal SDD functions either through direct contact with the I $\kappa$ B $\alpha$  substrate and/or through allosteric action on the KD to direct the specificity of IKK2 toward I $\kappa$ B $\alpha$  residues S32 and S36. In support of this hypothesis, Liu et al., when analyzing their recently published 2.8 Å X-ray crystal structure of an asymmetric dimer of human IKK2, identified a possible substrate peptide binding pocket within a crevice created by the KD and proximal SDD.<sup>24</sup> Future studies aimed at understanding how this domain arrangement affects substrate specificity and its potential as a target for drug development are underway.

We recently published experimental data, based on our own X-ray crystal structure of active human IKK2, in support of a regulatory model through which raising the local concentration of the enzyme promotes its spontaneous activation via oligomerization-dependent trans autophosphorylation.<sup>23</sup> Central to this hypothesis are the interactions observed between IKK2 dimers in the crystal. The open IKK2 dimer conformation permits interaction between neighboring dimers through a V-shaped interface involving portions of the KD, ULD, and proximal SDD. This interaction, in turn, stabilizes IKK2 in a conformation that can support KD–KD interactions and presumably trans autophosphorylation (Figure 1). As IKK2 dimerization relies exclusively on the distal SDD, generation of the stable, catalytically active IKK2<sup>mono</sup> enzyme has enabled further validation of this IKK2 activation mechanism.

Dimerization of IKK2 has been shown to be an absolute requirement for its activity in cells.<sup>15,22,32</sup> What is not clear from these studies, however, is whether blocking dimerization abolishes the potential for IKK2 to become active or whether it simply decreases the effective IKK2 concentration and consequently the probability of trans autophosphorylation. The involvement of V-shaped and KD–KD interfaces in IKK2 activation suggests that IKK2<sup>mono</sup>, which maintains these regions intact, should support trans autophosphorylation *in vitro*. In this study, we observe that this is, in fact, the case. We observe that the IKK2<sup>mono</sup> activation loop becomes phosphorylated spontaneously when expressed and purified from baculovirus-infected Sf9 insect cell suspensions. This is also true of dimeric IKK2 enzymes, suggesting that either the infected Sf9 cell environment or the level of IKK2 overexpression is sufficient to support its activation via trans

autophosphorylation. Strikingly, when residues that mediate the V-shaped or KD–KD interfaces are mutated, there is a complete loss of activation loop phosphorylation signal and consequently minimal activity toward I $\kappa$ B $\alpha$ . This loss in IKK2 trans autophosphorylation potential can then be partially recovered by increasing the concentration of the mutated IKK2 monomers.

Taken together, these experiments with an engineered monomeric IKK2 enzyme support an IKK2 activation mechanism in which the principal upstream event is to effectively increase the local concentration of IKK2 dimers. IKK2 dimers can then rapidly associate through V-shaped and KD–KD interfaces and become active via trans autophosphorylation. Under standard activation conditions, polyubiquitin chains induce IKK2 proximity through their noncovalent interaction with the NEMO subunit of IKK. However, this regulated process can be circumvented by other cellular events that drive IKK2 oligomerization.

## AUTHOR INFORMATION

### Corresponding Author

\*Phone: (619) 594-1606. E-mail: thuxford@mail.sdsu.edu.

### Present Address

§(J.D.S.) Novartis Institutes for Biomedical Research, 4560 Horton Street, Emeryville, California 94608, United States.

### Funding

This research was supported by NIH/NCI grant R01 CA141722 to G.G. and American Cancer Society grant RSG-08-287-01-GMC to T.H. A.V.H. is an Arne N. Wick predoctoral fellowship recipient. Biochemistry research at SDSU is supported in part by the California Metabolic Research Foundation.

### Notes

The authors declare no competing financial interest.

## ACKNOWLEDGMENTS

We thank M. P. Thompson and N. C. Gianneschi for SEC-MALLS, M. E. Lokensgard and J. J. Love for CD spectroscopy, S. Polley for helpful discussion, and V. Cardova for critical reading of the manuscript.

## ABBREVIATIONS USED

CD, circular dichroism; I $\kappa$ B, inhibitor of NF- $\kappa$ B; IKK, I $\kappa$ B kinase; HTLV, human T-lymphotropic virus; IL-1, interleukin-1; KSHV, Kaposi's sarcoma-associated herpesvirus; LPS, lipopolysaccharide; NF- $\kappa$ B, nuclear factor of  $\kappa$  light chain gene enhancer in B cells; SEC–MALLS, size-exclusion chromatography–multiangle laser light scattering; TNF- $\alpha$ , tumor necrosis factor  $\alpha$

## REFERENCES

- (1) Rothwarf, D. M., Zandi, E., Natoli, G., and Karin, M. (1998) IKK $\gamma$  is an essential regulatory subunit of the I $\kappa$ B kinase complex. *Nature* 395, 297–300.
- (2) Karin, M., and Ben-Neriah, Y. (2000) Phosphorylation meets ubiquitination: The control of NF- $\kappa$ B activity. *Annu. Rev. Immunol.* 18, 621–663.
- (3) Israël, A. (2010) The IKK complex, a central regulator of NF- $\kappa$ B activation. *Cold Spring Harbor Perspect. Biol.* 2, a000158-1–a000158-14.
- (4) Rudolph, D., Yeh, W. C., Wakeham, A., Rudolph, B., Nallainathan, D., Potter, J., Elia, A. J., and Mak, T. W. (2000) Severe

liver degeneration and lack of NF- $\kappa$ B activation in NEMO/IKK $\gamma$ -deficient mice. *Genes Dev.* 14, 854–862.

(5) Delhase, M., Hayakawa, M., Chen, Y., and Karin, M. (1999) Positive and negative regulation of I $\kappa$ B kinase activity through IKK $\beta$  subunit phosphorylation. *Science* 284, 309–313.

(6) Ninomiya-Tsuji, J., Kishimoto, K., Hiyama, A., Inoue, J., Cao, Z., and Matsumoto, K. (1999) The kinase TAK1 can activate the NIK-I $\kappa$ B as well as the MAP kinase cascade in the IL-1 signalling pathway. *Nature* 398, 252–256.

(7) Vig, E., Green, M., Liu, Y., Donner, D. B., Mukaida, N., Goebel, M. G., and Harrington, M. A. (1999) Modulation of tumor necrosis factor and interleukin-1-dependent NF- $\kappa$ B activity by mPLK/IRAK. *J. Biol. Chem.* 274, 13077–13084.

(8) Wang, C., Deng, L., Hong, M., Akkaraju, G. R., Inoue, J., and Chen, Z. J. (2001) TAK1 is a ubiquitin-dependent kinase of MKK and IKK. *Nature* 412, 346–351.

(9) Yang, J., Lin, Y., Guo, Z., Cheng, J., Huang, J., Deng, L., Liao, W., Chen, Z., Liu, Z., and Su, B. (2001) The essential role of MEKK3 in TNF-induced NF- $\kappa$ B activation. *Nat. Immunol.* 2, 620–624.

(10) Bagnier, C., Ageichik, A. V., Cronin, N., Wallace, B., Collins, M., Boshoff, C., Waksman, G., and Barrett, T. (2008) Crystal structure of a vFlip-IKK $\gamma$  complex: Insights into viral activation of the IKK signalosome. *Mol. Cell* 30, 620–631.

(11) Field, N., Low, W., Daniels, M., Howell, S., Daviet, L., Boshoff, C., and Collins, M. (2003) KSHV vFLIP binds to IKK $\gamma$  to activate IKK. *J. Cell Sci.* 116, 3721–3728.

(12) Huang, G. J., Zhang, Z. Q., and Jin, D. Y. (2002) Stimulation of IKK $\gamma$  oligomerization by the human T-cell leukemia virus oncoprotein Tax. *FEBS Lett.* 531, 494–498.

(13) Jin, D. Y., Giordano, V., Kibler, K. V., Nakano, H., and Jeang, K. T. (1999) Role of adapter function in oncoprotein-mediated activation of NF- $\kappa$ B. Human T-cell leukemia virus type I Tax interacts directly with I $\kappa$ B kinase  $\gamma$ . *J. Biol. Chem.* 274, 17402–17405.

(14) Miller, B. S., and Zandi, E. (2001) Complete reconstitution of human I $\kappa$ B kinase (IKK) complex in yeast. Assessment of its stoichiometry and the role of IKK $\gamma$  on the complex activity in the absence of stimulation. *J. Biol. Chem.* 276, 36320–36326.

(15) Zandi, E., Chen, Y., and Karin, M. (1998) Direct phosphorylation of I $\kappa$ B by IKK $\alpha$  and IKK $\beta$ : Discrimination between free and NF- $\kappa$ B-bound substrate. *Science* 281, 1360–1363.

(16) Xia, Z. P., Sun, L., Chen, X., Pineda, G., Jiang, X., Adhikari, A., Zeng, W., and Chen, Z. J. (2009) Direct activation of protein kinases by unanchored polyubiquitin chains. *Nature* 461, 114–119.

(17) DiDonato, J., Mercurio, F., Rosette, C., Wu-Li, J., Suyang, H., Ghosh, S., and Karin, M. (1996) Mapping of the inducible I $\kappa$ B phosphorylation sites that signal its ubiquitination and degradation. *Mol. Cell. Biol.* 16, 1295–1304.

(18) DiDonato, J. A., Hayakawa, M., Rothwarf, D. M., Zandi, E., and Karin, M. (1997) A cytokine-responsive I $\kappa$ B kinase that activates the transcription factor NF- $\kappa$ B. *Nature* 388, 548–554.

(19) Chariot, A. (2009) The NF- $\kappa$ B-independent functions of IKK subunits in immunity and cancer. *Trends Cell Biol.* 19, 404–413.

(20) Li, Q., Van Antwerp, D., Mercurio, F., Lee, K. F., and Verma, I. M. (1999) Severe liver degeneration in mice lacking the I $\kappa$ B kinase 2 gene. *Science* 284, 321–325.

(21) Li, Z. W., Chu, W., Hu, Y., Delhase, M., Deerinck, T., Ellisman, M., Johnson, R., and Karin, M. (1999) The IKK $\beta$  subunit of I $\kappa$ B kinase (IKK) is essential for nuclear factor  $\kappa$ B activation and prevention of apoptosis. *J. Exp. Med.* 189, 1839–1845.

(22) Xu, G., Lo, Y. C., Li, Q., Napolitano, G., Wu, X., Jiang, X., Dreano, M., Karin, M., and Wu, H. (2011) Crystal structure of inhibitor of  $\kappa$ B kinase  $\beta$ . *Nature* 472, 325–330.

(23) Polley, S., Huang, D. B., Hauenstein, A. V., Fusco, A. J., Zhong, X., Vu, D., Schröfelbauer, B., Kim, Y., Hoffmann, A., Verma, I. M., Ghosh, G., and Huxford, T. (2013) A structural basis for I $\kappa$ B kinase 2 activation via oligomerization-dependent trans auto-phosphorylation. *PLoS Biol.* 11, e1001581-1–e1001581-13.

(24) Liu, S., Misquitta, Y. R., Olland, A., Johnson, M. A., Kelleher, K. S., Kriz, R., Lin, L. L., Stahl, M., and Mosyak, L. (2013) Crystal

structure of a human I $\kappa$ B kinase  $\beta$  asymmetric dimer. *J. Biol. Chem.* 288, 22758–22767.

(25) Shaul, J. D., Farina, A., and Huxford, T. (2008) The human IKK $\beta$  subunit kinase domain displays CK2-like phosphorylation specificity. *Biochem. Biophys. Res. Commun.* 374, 592–597.

(26) Whitmore, L., and Wallace, B. A. (2008) Protein secondary structure analyses from circular dichroism spectroscopy: Methods and reference databases. *Biopolymers* 89, 392–400.

(27) Sreerama, N., Veenyaninov, S. Y., and Woody, R. W. (1999) Estimation of the number of  $\alpha$ -helical and  $\beta$ -strand segments in proteins using circular dichroism spectroscopy. *Protein Sci.* 8, 370–380.

(28) Janes, R. W. (2009) Reference datasets for protein circular dichroism and synchrotron radiation circular dichroism spectroscopic analyses, In *Modern Techniques for Circular Dichroism and Synchrotron Radiation Circular Dichroism Spectroscopy* (Wallace, B. A., and Janes, R. W., Eds.) pp 183–201, IOS Press, Washington, DC.

(29) Larabi, A., Devos, J. M., Ng, S. L., Nanao, M. H., Round, A., Maniatis, T., and Panne, D. (2013) Crystal structure and mechanism of activation of TANK-binding kinase 1. *Cell Rep.* 3, 734–746.

(30) Tu, D., Zhu, Z., Zhou, A. Y., Yun, C. H., Lee, K. E., Toms, A. V., Li, Y., Dunn, G. P., Chan, E., Thai, T., Yang, S., Ficarro, S. B., Marto, J. A., Jeon, H., Hahn, W. C., Barbie, D. A., and Eck, M. J. (2013) Structure and ubiquitination-dependent activation of TANK-binding kinase 1. *Cell Rep.* 3, 747–758.

(31) Jiang, X., and Chen, Z. J. (2012) The role of ubiquitylation in immune defence and pathogen evasion. *Nat. Rev. Immunol.* 12, 35–48.

(32) Zandi, E., Rothwarf, D. M., Delhase, M., Hayakawa, M., and Karin, M. (1997) The I $\kappa$ B kinase complex (IKK) contains two kinase subunits, IKK $\alpha$  and IKK $\beta$ , necessary for I $\kappa$ B phosphorylation and NF- $\kappa$ B activation. *Cell* 91, 243–252.

(33) Manning, G., Whyte, D. B., Martinez, R., Hunter, T., and Sudarsanam, S. (2002) The protein kinase complement of the human genome. *Science* 298, 1912–1934.

(34) Huse, M., and Kuriyan, J. (2002) The conformational plasticity of protein kinases. *Cell* 109, 275–282.

(35) Nolen, B., Taylor, S., and Ghosh, G. (2004) Regulation of protein kinases; controlling activity through activation segment conformation. *Mol. Cell* 15, 661–675.

(36) Chen, Z., Hagler, J., Palombella, V. J., Melandri, F., Scherer, D., Ballard, D., and Maniatis, T. (1995) Signal-induced site-specific phosphorylation targets I $\kappa$ B $\alpha$  to the ubiquitin-proteasome pathway. *Genes Dev.* 9, 1586–1597.

(37) Chen, Z. J. (2012) Ubiquitination in signaling to and activation of IKK. *Immunol. Rev.* 246, 95–106.

(38) Wertz, I. E., and Dixit, V. M. (2010) Signaling to NF- $\kappa$ B: Regulation by ubiquitination. *Cold Spring Harbor Perspect. Biol.* 2, a003350-1–a003350-19.